

Electrical Characteristics of InAlAs/InGaAs/InAlAs Pseudomorphic High Electron Mobility Transistors under Sub-Bandgap Photonic Excitation

H.T. Kim and D. M. Kim*

Abstract— Electrical gate and drain characteristics of double heterostructure InAlAs/InGaAs pseudomorphic HEMTs have been investigated under sub-bandgap photonic excitation ($h\nu < E_g$). Drain (V_{DS})-, gate (V_{GS})-, and optical power (P_{opt})-dependent variation of the abnormal gate leakage current and associated physical mechanisms in the PHEMTs have been characterized. Peak gate voltage ($V_{GS,p}$) and the onset voltage for the impact ionization ($V_{GS,II}$) have been extracted and empirical model for their dependence on the V_{DS} and P_{opt} have been proposed. Anomalous gate and drain current, both under dark and under sub-bandgap photonic excitation, have been modeled as a parallel connection of high performance PHEMT with a poor satellite FET as a parasitic channel. Sub-bandgap photonic characterization, as a function of the optical power with $h\nu=0.799\text{eV}$, has been comparatively combined with those under dark condition for characterizing the bell-shaped negative humps in the gate current and subthreshold drain leakage under a large drain bias.

Index Terms— HEMT, HFET, gate current, physical mechanism, resonant tunneling, real space transfer, positive hump

I. INTRODUCTION

InP-based pseudomorphic high electron mobility transistors (PHEMTs) became important with the growing applications in low-noise and low-power microwave & millimeter-wave integrated circuits. InP-based PHEMTs are superior in performance to conventional GaAs-based HEMTs due to the significantly higher low-field channel electron mobility with reduced parasitic resistances. They, however, often suffer from poor breakdown, gate leakage, and subthreshold drain characteristics with the inherent small bandgap of the channel layer in the structure [1-13]. There has been much effort to improve both the gate Schottky barrier and the breakdown characteristics through modification of the epitaxial layers and fabrication processes. There have also been considerable efforts on the improvement of the gate and drain leakage characteristics that are closely related to the noise figure, breakdown characteristics, and high-frequency performance of InP-based PHEMTs. Physical mechanisms on the breakdown and abnormal gate&drain leakage currents in PHEMTs include thermal generation & recombination (G-R), impact ionization, thermionic field emission, tunneling, real space transfer, and/or combination of thereof [1-5, 10,11,14].

In this work, we demonstrate a new optoelectronic technique for characterizing the dominant mechanisms of abnormal current-voltage properties in InAlAs/InGaAs PHEMTs. We employed a sub-bandgap optical source with $h\nu=0.799\text{eV}$ ($\lambda=1551\text{nm}$), which is non-responsive to epitaxial layers except the InGaAs channel

Manuscript received August 1, 2003; revised August 20, 2003.

H.T. Kim and D. M. Kim are with School of Electrical Engineering, Kookmin University 861-1 Jungnung-dong, Sungbuk-gu, Seoul, 136-702, Korea

Tel : +82-2-910-4719, Fax : +82-2-910-4449

E-mail : dmkim@kookmin.ac.kr

layers, modulating the optical power (P_{opt}) from dark to $P_{opt}=2.51\text{mW}(+4\text{dbm})$.

II. FABRICATION AND CURRENT-VOLTAGE CHARACTERISTICS OF PHEMTs UNDER DARK

The MBE-grown epitaxial structure of the characterized double heterostructure InAlAs/InGaAs/InAlAs PHEMTs on InP wafer with a V-shaped gate

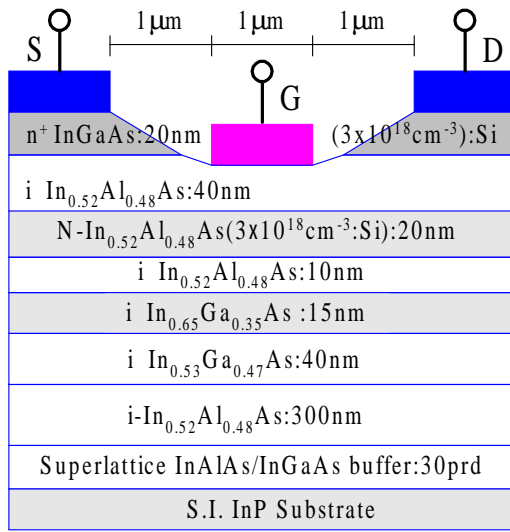
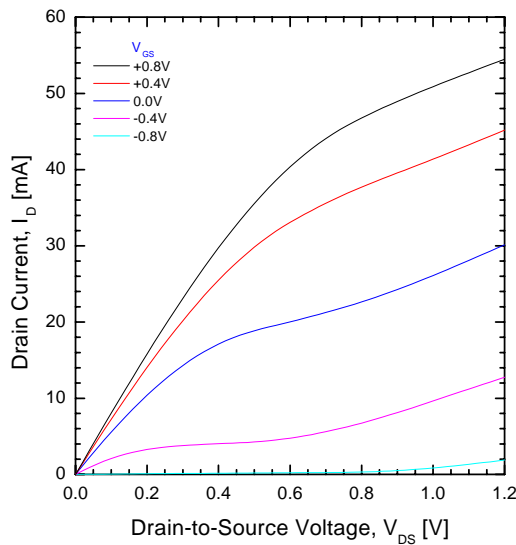
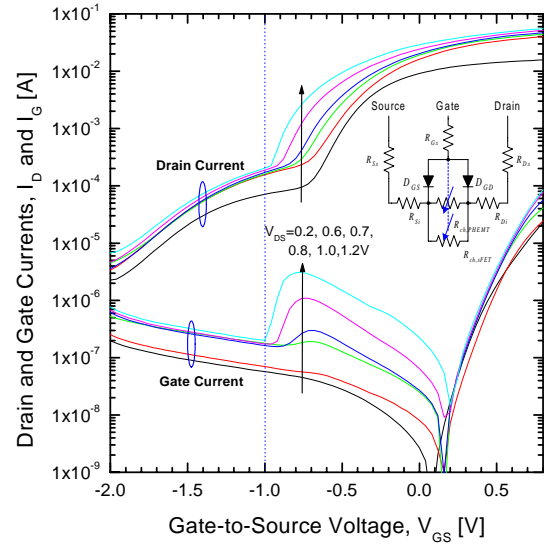


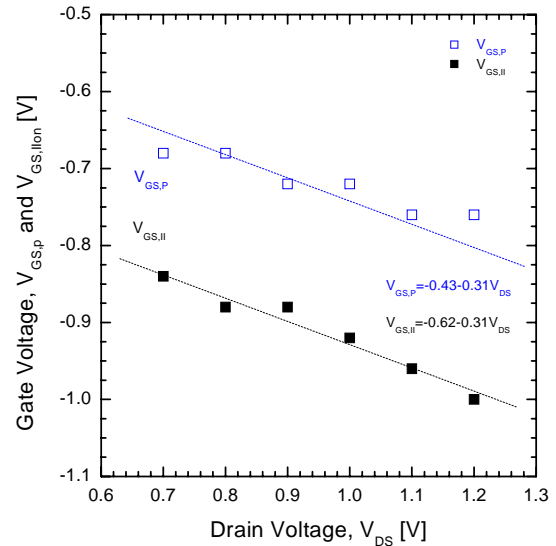
Fig. 1. Epitaxial structure and schematic energy band diagram of probed InAlAs/InGaAs PHEMTs with $W/L=200\mu\text{m}/1\mu\text{m}$ and $L_{gs}=L_{gd}=1\mu\text{m}$.



(a) I_D - V_{DS} characteristics under dark



(b) I_G - V_{DS} characteristics under dark (with an equivalent circuit as an insert)



(c) Peak- $(V_{GS,P})$ and onset-gate voltages ($V_{GS,II}$) of the impact ionization under dark.

Fig. 2. Drain and gate current-voltage characteristics of PHEMTs under dark.

($W=2\times 100\mu\text{m}$, $L_g=1.0\mu\text{m}$) is shown in Fig. 1. Wet chemical etching and conventional optical lithography processes were employed for the fabrication of PHEMTs. Between the undoped $\text{In}_{0.52}\text{Al}_{0.48}\text{As}$ barrier layers, lattice-matched $\text{In}_{0.52}\text{Ga}_{0.47}\text{As}$ ($E_g\sim 0.62\text{eV}$) and pseudomorphic $\text{In}_{0.65}\text{Ga}_{0.35}\text{As}$ ($E_g\sim 0.75\text{eV}$) layers were sandwiched as a high mobility conducting channel in the PHEMT. We also note that the InGaAs channel layers

are photoresponsive for the band-to-band excess carrier generation to the optical source with the sub-bandgap photon energy ($h\nu=0.799\text{eV}$) while InP and InAlAs layers are transparent to it. We may also expect that there is a spatial (real space) transfer of carriers from the channel layer to adjacent layers overcoming the band discontinuities in the conduction and valence bands ($\Delta E_C\sim 0.5\text{eV}$, $\Delta E_V\sim 0.2\text{eV}$ in $\text{In}_{0.52}\text{Al}_{0.48}\text{As}/\text{In}_{0.65}\text{Ga}_{0.35}\text{As}$ heterostructure).

The current-voltage characteristics of PHEMTs without optical excitation ($P_{opt}=0\text{mW}$) were probed at room temperature ($T=300\text{K}$), and, the drain and gate currents (I_D and I_G) are shown in Fig. 2(a) and (b) as a function of the drain and gate voltages (V_{DS} and V_{GS}): (I_D - V_{DS} curve; $V_{GS}=-1.2\sim+0.8\text{V}$ and I_G - V_{GS} curve; $V_{DS}=0.1\sim 1.1\text{V}$). The saturated drain current (I_{DSS}), the maximum transconductance ($g_{m,max}$), and the threshold voltage (V_T) under dark condition ($P_{opt}=0\text{ mW}$) were measured to be $I_{DSS}=150\text{ mA/mm}$, $g_{m,max}=220\text{ mS/mm}$ (at $V_{DS}=1.2\text{V}$), and $V_T\cong -0.95\text{V}$, respectively. As typically observed in short-channel InP-based PHEMTs, a channel length modulation was also observed. Typical values of the common-source current gain cut-off frequency (f_T) and maximum oscillation frequency (f_{max}), from devices on the same wafer, were measured to be $f_T=30\text{GHz}$ and $f_{max}=48\text{GHz}$, respectively.

Under low drain voltages, the reverse gate current in the I_G - V_{GS} curve is mainly caused by the thermionic-field emission and the field-assisted tunneling in addition to the thermal generation of carriers in the depletion region under the gate [1-5]. We note that the negative bell-shaped gate leakage is observed in the I_G - V_{GS} characteristics under high drain voltage over $V_{DS}>0.7\text{V}$. This is known to be caused predominantly by the successive collection of generated holes due to the impact ionization by hot channel electrons under a high electric field [1-2].

From the $I_D^{1/2}$ - V_{GS} characteristics, it seems that two PHEMTs, with two different threshold voltages and transconductances, are connected in parallel. Main contribution of the PHEMT (region-A), with a high conductivity InGaAs channel layer, has $V_T\sim -0.95\text{V}$ while a poor performance satellite FET (sFET: region-B), probably due to a parasitic conduction layer as a MESFET with an InAlAs doped layer, has $V_{Ts}\sim -2.0\text{V}$ under dark condition. Equivalent circuit of the device

under test is shown in Fig. 2(b) as an insert.

The gate current can be grouped into 3 distinct regions. In the region-A, the gate current is expected to be governed by the minority carrier diffusion current ($I_{G,S}$), thermal generation current ($I_{G,GnR}$) in the depletion region, and a possible contribution of the tunneling current ($I_{G,Tunnel}$) as well as the impact ionization ($I_{G,II}$) under high drain bias. Under low drain bias, main contribution of the gate current in this region-A is due to $I_{G,S}$ and $I_{G,GnR}$. However, it is predominantly governed by the impact ionization ($I_{G,II}$) under high drain bias above $V_{DS}>0.7\text{V}$ which is expected to depend strongly on the device structure. In the region-B, on the other hand, the reverse gate leakage current is expected to be governed by the thermionic field emission ($I_{G,TFE}$) component in addition to the thermally generated current ($I_{G,GnR}$) in the extended depletion with elevated reverse gate bias. In the region-C with a positive gate bias, the main contribution of the gate current is expected to be the thermionic emission ($I_{G,TE}$) due to enhanced injection of carriers over the built-in energy barrier and, therefore, a quasi-exponential increase of the gate current is observed. In the region-B, the parasitic transistor sFET governs the drain leakage current while the PHEMT with InGaAs as a channel layer is the dominant current-controlling path in this structure. The onset of the impact ionization can be explained by the onset/turn-on of the PHEMT overcoming the satellite FET as a parasitic leakage path with a poor channel conductivity.

The peak gate voltage ($V_{GS,P}$ at which the reverse gate current shows a peak value) and the onset-gate voltage of the impact ionization ($V_{GS,II}$ at which the reverse gate current starts to abruptly increase probably due to the impact ionization under high drain voltage) are summarized in Fig. 2(c) as a function of V_{DS} under dark condition. They show $V_{GS,P} = -0.43 - 0.31V_{DS}$ and $V_{GS,II} = -0.62 - 0.31V_{DS}$ as a linear function of V_{DS} with the same V_{DS} -dependence (slope= -0.31 V^{-1}). This is mainly due to the accelerated electric field and increased probability of impact ionization resulting a parallel shift of them with V_{DS} . Peak gate voltage $V_{GS,P}$ shows a parallel shift from the $V_{GS,II}$ because the impact ionization and resulting the gate current depend on both the number of available carriers and the strength of the accelerating electric field for high kinetic energy in the conducting InGaAs channel layer.

III. SUB-BANDGAP OPTOELECTRONIC CHARACTERIZATION OF THE GATE CURRENT

Optoelectronic characteristics of PHEMTs under a sub-bandgap photonic excitation were probed as a function of the optical power and compared with those under dark condition. We observed that the transconductance ($g_m = \partial I_d / \partial V_{gs}$) is observed to be $g_{m,max} = 220$ mS/mm and independent of the optical power over $P_{opt} = 0 \sim 2.51$ mW (+4dbm). The cleaved optical fiber, for delivering the optical power, has an illumination

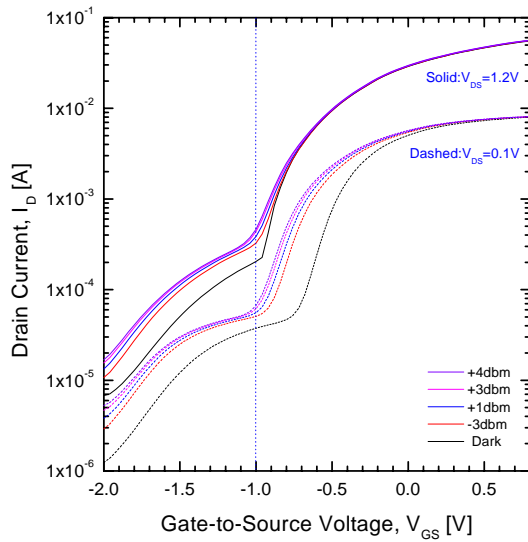
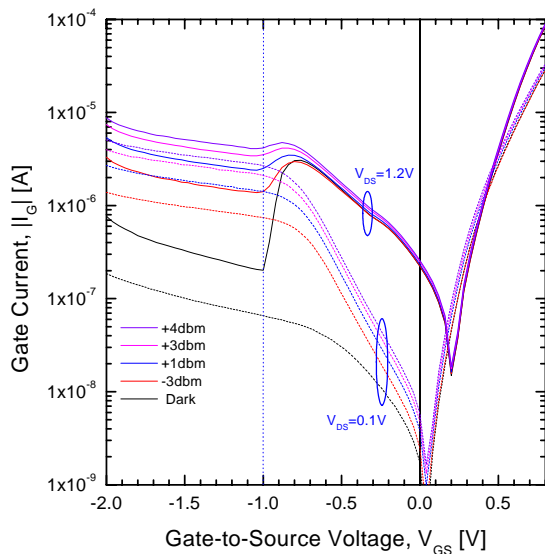
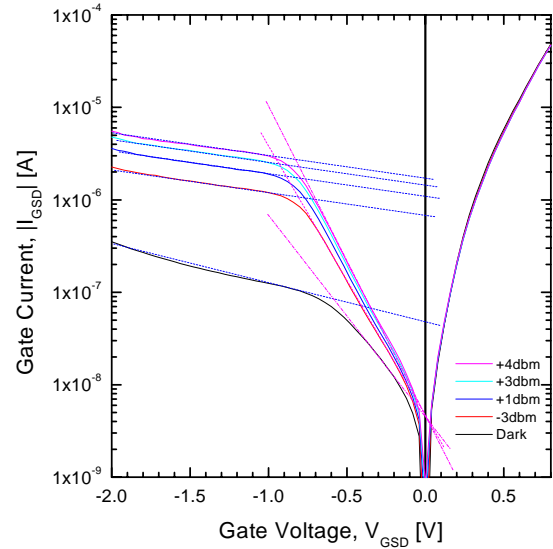


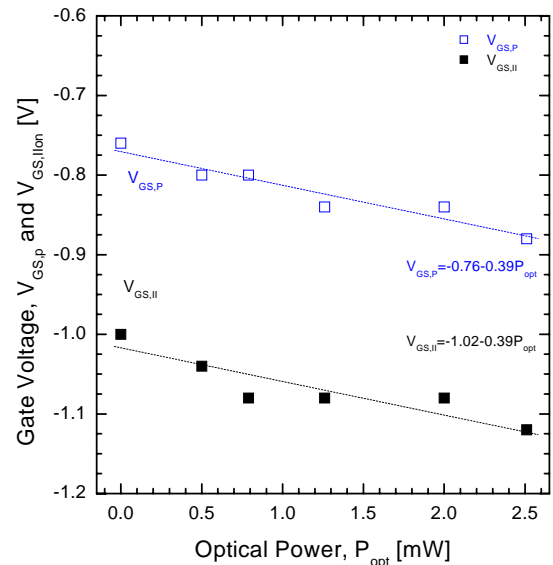
Fig. 3. Drain current-gate voltage characteristics of PHEMTs under optical excitation ($P_{opt} = 0 \sim 2.51$ mW with $h\nu = 0.799$ eV).



(a) $I_G(V_{GS}, P_{opt})$: gate leakage current in the PHEMT with a specific drain voltage



(b) $I_{GSD}(V_{GSD}, P_{opt})$: gate current of PHEMTs with a short-circuited source & drain.



(c) Peak- (V_{GSP}) and onset-gate voltages ($V_{GS,on}$) of the impact ionization under illumination.

Fig. 4. Gate leakage current-voltage characteristics of pHEMTs under optical excitation ($P_{opt} = 0 \sim 2.51$ mW with $h\nu = 0.799$ eV).

diameter $\phi \sim 60 \mu\text{m}$ and covers the surface of the PHEMT under characterization. We note that only the InGaAs channel layer, among all other layers in the InAlAs/InGaAs PHEMT, is optically responsive for the band-to-band excitation to the optical input with a sub-bandgap photon $h\nu = 0.799$ eV. We also note that traps and interface states at the heterojunctions in the PHEMTs are also photoresponsive and may contribute to the gate and drain

currents, especially with a subthreshold gate bias, under this sub-bandgap photonic excitation [6].

Drain current response (I_D - V_{GS}) under a sub-bandgap photonic excitation is shown in Fig. 3 as a function of the gate bias for $V_{DS}=0.1$ (linear mode) and $1.2V$ (saturation mode). We note that there is a significant change in the drain current with P_{opt} in the sub-threshold and negative gate bias ($V_{GS}<0V$) while a negligible change in the above-threshold drain current of the gate bias for both small ($V_{DS}=0.1V$) and large ($1.2V$) drain biases. This implies that carriers excited from the traps in the heterojunction interface may be partially responsible for this observation, especially in the subthreshold gate bias, under a sub-bandgap photonic excitation with $h\nu < E_g$.

Gate current characteristics (I_G - V_{GS}) under sub-bandgap photonic excitation are shown in Fig. 4(a) in parallel with a gate current in the diode configuration (short-circuited source and drain) of the PHEMT in Fig. 4(b). Contrary to the drain current, we observed a significant change in the gate current with P_{opt} in saturation region under a large drain bias while a negligible change in the linear region under a small drain bias. We note that the negative humps under negative gate bias and large drain bias under dark condition is disappeared in the I_G - V_{GS} characteristics with a sub-bandgap photonic excitation over $P_{opt}=-3\text{dbm}$ to $+4\text{dbm}$. P_{opt} -dependent change of the peak and onset voltages ($V_{GS,PO}$ and $V_{GS,II}$) of the PHEMT as a function of the

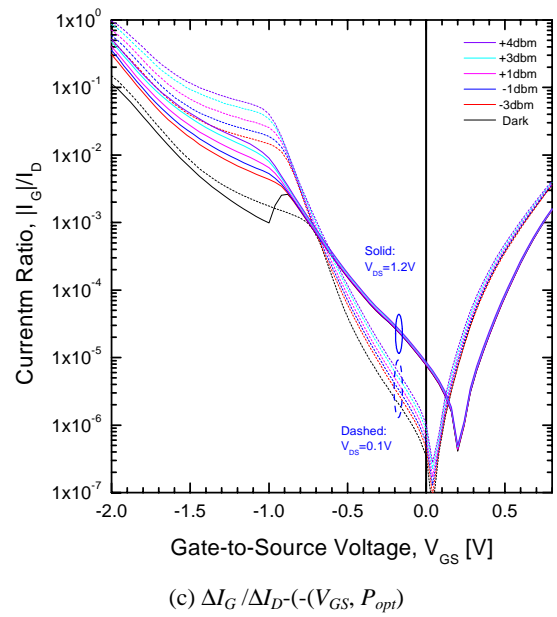
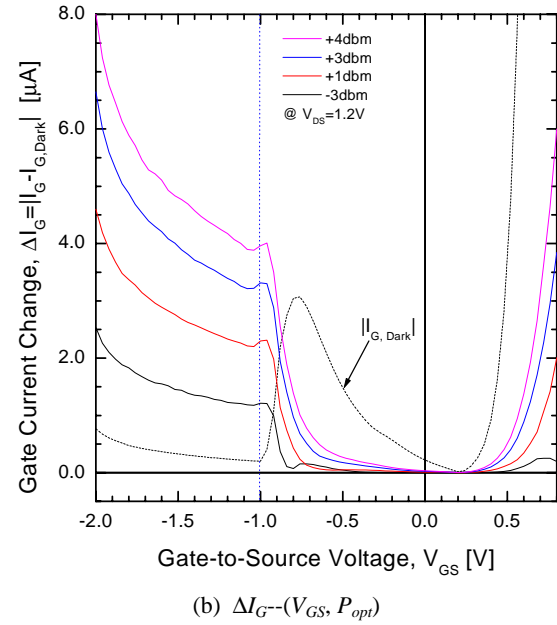
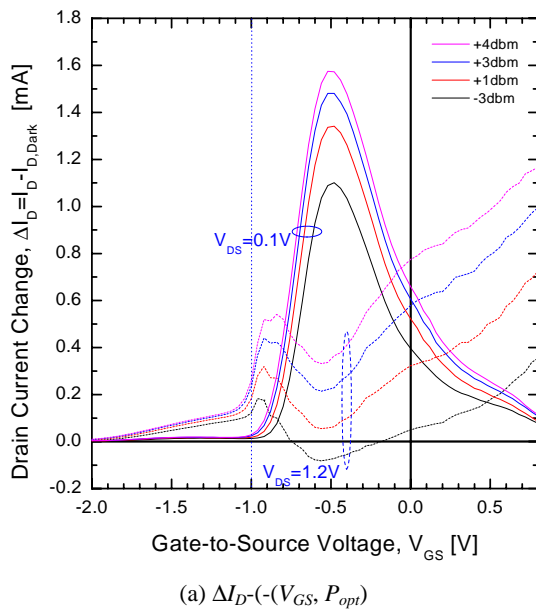


Fig. 5. Drain and gate current change with optical excitation ($P_{opt}=0.5\sim 2.51\text{mW}$) at $V_{DS}=1.2V$ compared with dark condition ($\Delta I_D=I_D-I_{D,Dark}$, $\Delta I_G=I_G-I_{G,Dark}$).

optical excitation in Fig. 4 (c).

Under optical input with P_{opt} in mW, they show $V_{GS,PO} = -0.76 - 0.39P_{opt}$ and $V_{GS,II} = -1.02 - 0.39P_{opt}$ as a linear function of P_{opt} and the same P_{opt} -dependence (Slope= -0.39 mW^{-1}) is observed for both $V_{GS,P}$ and $V_{GS,II}$. From this, we obtain a parallel/linear shift of $V_{GS,P}$ and the onset gate voltage $V_{GS,II}$ with the

optical power. This is expected to be due to the photovoltaic effect under the sub-bandgap optical excitation of excess carriers in the InGaAs channel and additional excess carriers excited from the interface traps at the heterojunction interfaces. We also note that there is a significant shift of the threshold voltage and increase of the drain current in sFET and PHEMT with the photonic excitation under low V_{DS} while a considerable change of the drain current in sFET, but negligible change of V_T and I_D under large drain bias. This is also expected to be partially due to the photonic modulation of the parasitic resistances under sub-bandgap optical illumination. This is also observed in the I_D - V_{DS} curves of PHEMT under photonic excitation.

From this observation, the physical mechanism generating the negative bell-shaped gate current is not solely attributed to the impact ionization. If the main cause of the negative bell-shaped gate leakage current is only the impact ionization, the gate current at the peak current and the onset of the impact ionization in the region-A should be considerably increased due to the contribution of the optically pumped excess channel carriers under optical input. However, as shown in Fig. 5 (a), (b), and (c), the gate and drain current under optical input doesn't show significant change in the region-A. There is no close relation between the change in the gate current and that in the drain current. We see significant

change of the gate current in the region-B while considerable change of the drain current in the region-A under sub-bandgap photonic excitation.

We also investigated the ideality factor of the gate current in each region and summarized in Table I for (a) a low drain bias : $V_{DS}=0.1V$ and (b) high drain bias : $V_{DS}=1.2V$. The gate current in the region-A (I_{GA}) and the region-B (I_{GB}) can be modeled with the ideality factors (η_A & η_B) and the saturation currents (I_{GAo} & I_{GBo}) as $I_{GA} = -I_{GAo} \exp(-V_{GS}/\eta_A V_{th})$ and $I_{GB} = -I_{GBo} \exp(-V_{GS}/\eta_B V_{th})$.

Under low V_{DS} , the saturation current (I_{GAo}) of the reverse gate leakage in the region-A is almost fixed at $I_{GAo} \sim 4.3 \times 10^{-9} [A]$ (for $P_{opt} = \text{dark} \sim +4\text{dbm}$) while the ideality factor (η_A) is significantly modulated by the optical input ($\eta_{A|\text{dark}} = 7.58 \sim \eta_{A|+4\text{dbm}} = 4.95$). However, both the reverse saturation current (I_{GBo}) and the ideality factor (η_B) in the region-B are significantly modulated ($I_{GBo|\text{dark}} = 4.5 \times 10^{-8} [A] \sim I_{GBo|+4\text{dbm}} = 1.7 \times 10^{-6} [A]$, $\eta_{B|+4\text{dbm}} = 41.0 \sim \eta_{B|\text{dark}} = 66.7$) by the sub-bandgap optical excitation. Under large V_{DS} , P_{opt} -dependent variations of the reverse gate saturation current and the ideality factors show the same dependence on the optical power as those under low drain bias.

IV. CONCLUSION

Optoelectronic gate and drain characteristics of InAlAs/InGaAs pseudomorphic HEMTs have been investigated as a function of sub-bandgap optical power with $h\nu=0.799\text{eV}$. Abnormal gate leakage under reverse bias, including the bell-shaped negative humps in the I_G - V_{GS} curves under a large drain bias, and associated physical mechanisms were characterized. V_{DS} -, V_{GS} -, and P_{opt} -dependent variation of the anomalous gate and subthreshold drain current, and associated physical mechanisms in the PHEMTs have been characterized. Peak gate voltage and the onset voltage for the impact ionization have been extracted and their linear relationship with V_{DS} and P_{opt} have been empirically modeled. Electrical characteristics under dark and sub-bandgap photonic characterization, as a function of P_{opt} with $h\nu=0.799\text{eV}$, have been comparatively combined and related mechanisms have been analyzed. We expect

Table I. Ideality factors (η) and saturation currents as a function of the photonic excitation (P_{opt}) in the gate current in each region modeled as $I_{GA} = -I_{GAo} \exp(-V_{GS}/\eta_A V_{th})$ and $I_{GB} = -I_{GBo} \exp(-V_{GS}/\eta_B V_{th})$.

(a) Under low V_{DS} (0V or source-and-drain short-circuited)

	Dark	-3dbm	-1dbm	+1dbm	+4dbm
I_{GAo}	4.3×10^{-9}	4.3×10^{-9}	4.3×10^{-9}	4.3×10^{-9}	4.3×10^{-9}
η_A	7.58	5.66	5.33	5.11	4.95
I_{GBo}	4.5×10^{-8}	6.5×10^{-7}	1.1×10^{-6}	1.4×10^{-6}	1.7×10^{-6}
η_B	41.0	66.7	66.7	66.7	66.7

(b) Under high V_{DS} (1.2V)

	Dark	-3dbm	-1dbm	+1dbm	+4dbm
I_{GAo}	$\sim 3.0 \times 10^{-7}$	$\sim 3.0 \times 10^{-7}$	$\sim 3.0 \times 10^{-7}$	$\sim 3.0 \times 10^{-7}$	$\sim 3.0 \times 10^{-7}$
η_A	12.3	12.1	11.9	11.63	11.01
I_{GBo}	6.7×10^{-8}	7.1×10^{-7}	1.2×10^{-6}	1.5×10^{-6}	2.1×10^{-6}
η_B	36.0	63.4	63.4	63.4	63.4

that this sub-bandgap photonic characterization can be applied to the investigation of physical mechanisms related to the gate leakage, the subthreshold drain leakage, and the interface states at the heterojunction of PHEMTs.

V. ACKNOWLEDGEMENT

This work was supported by the Korea Research Foundation under Grant KRF-2001-041-E00166 and by KOSEF through the MINT Research Center at Dongguk University.

REFERENCES

- [1] S. Maruno, Y. Abe, T. Ozeki, T. Nakamoto, and N. Yoshida, "Isothermal capacitance transient spectroscopy of pseudomorphic high-electron-mobility transistors," *Appl. Phys. Lett.*, Vol. 82, pp. 3339-3341, May 2003.
- [2] S.D. Cho, H.T. Kim, and D.M. Kim, "Physical mechanisms on the abnormal gate leakage currents in pseudomorphic high electron mobility transistors," *IEEE Trans. Electron Devices*, Vol.50, no.4, pp.1148-1152, April 2003.
- [3] R. Menozzi, "Hot electron effects and degradation of GaAs and InP HEMTs for microwave and millimetre-wave applications," *Semiconductor Science Technology*, Vol. 13, pp. 1053-1063, Oct. 1998.
- [4] S. Takamiya, M. Harayama, T. Sugimura, T. Tsuzuku, T. Taya, K. Iiyama, and S. Hashimoto, "Reverse currents of Schottky gates of III-V MESFET/HEMTs: field emission and tunnel currents," *Solid-State Electronics*, Vol. 42, pp. 447-451, March 1998.
- [5] G. Meneghesso, A. Neviani, R. Oesterholt, M. Matloubian, T. Liu, J.J. Brown, C. Canali, and E. Zanoni, "On-state and off-state breakdown in GaInAs/InP composite-channel HEMT's with variable GaInAs channel thickness," *IEEE Trans. Electron Devices*, Vol. 46, pp.2-9, Jan. 1999.
- [6] R.T. Webster, S. Wu, and A.F.M. Anwar, "Impact ionization in InAlAs/InGaAs/InAlAs HEMT's," *IEEE Electron Device Lett.*, Vol.21, pp.193-195, May 2000.
- [7] D.-H. Kim, S.-W. Kim, S.-C. Hong, S.-W. Paek, J.-H. Lee, K.-W. Jung, and K.-S. Seo, "fabrication and characterization of 0.2 μ m InAlAs/InGaAs M-HEMT's with inverse step-graded InAlAs buffer on GaAs substrate," *J. Semiconductor Tech. and Science*, Vol.1, pp.111-115, 2001.
- [8] S. Takatani, H. Matsumoto, J. Shigeta, K. Ohshika, T. Yamashita, and M. Fukui, "Generation mechanism of gate leakage current due to reverse-voltage stress i-AlGaAs/n-GaAs HIGFET's," *IEEE Trans. Electron Devices*, Vol. 45, pp.14-20, Jan. 1998.
- [9] B. Georgescu, M.A. Py, A. Souifi, and G. Guilot, "New aspects and mechanism of kink effect in InAlAs/InGaAs/InP inverted HFET's," *IEEE Electron Device Lett.*, Vol. 19, pp.154-156, May 1998.
- [10] N. Labat, N. Saisset, A. Touboul, Y. Danto, P. Cova and F. Fantini, "Analysis of hot electron degradations in pseudomorphic HEMTs by DCTS and LF noise characterization," *Microelectronics Reliability*, Vol.37, pp. 1675-1678, Oct. 1997.
- [11] Y. C. Chou, G. P. Li, Y. C. Chen, C.S. Wu, K.K. Yu, and T. A. Midford, "Off-state breakdown effects on gate leakage current in power pseudomorphic AlGaAs/InGaAs HEMTs," *IEEE Electron Device Lett.*, Vol.18, pp. 479-481, Oct. 1996.
- [12] M. H. Somerville, J. A. del Alamo, and P. Saunier, "Off-state breakdown in power pHEMTs: the impact of the source," *IEEE Trans. Electron Devices*, Vol. 45, pp. 1883-1889, Sept. 1998.
- [13] D.-H. Kim, S.-J. Kim, Y.-H. Kim, S.-W. Kim, and K.-S. Seo, "40nm InGaAs HEMT's with 65% strained channel fabricated with damage-free SiO₂/SiN_x side-wall gate process," *J. Semiconductor Tech. and Science*, Vol.3, pp.27-32, 2003.
- [14] C.-L. Wu and W.-C. Hsu, "Enhanced resonant tunneling real-space transfer in δ -doped GaAs/InGaAs gated dual-channel transistors grown by MOCVD," *IEEE Trans. Electron Devices*, Vol. 43, pp. 207-212, Feb. 1996.



Hae Taek Kim received the B.S. and M.S. degrees in electronics engineering from the Kookmin University, Korea, in 1994 and 1996, respectively. He is currently pursuing the Ph.D. degree at the same university. His research interest includes design, modeling, and characterization of high performance semiconductor devices and integrated circuits with MOSFETs, HEMTs & HBTs, and nanostructure quantum effect devices.

He also works on the development and application of the photonic and optoelectronic microwave technique for the characterization of physical mechanisms in semiconductor devices.



Dong Myong Kim received the B.S. (magna cum laude) and M.S. degrees in electronics engineering from the Seoul National University, Korea, in 1986 and 1988, respectively, and the Ph.D. degree in electrical engineering from the University of Minnesota, Minneapolis, in 1993. In March 1993, he joined the

School of Electrical Engineering at the Kookmin University,

Korea, and is now an Associate Professor. His research interest includes design, modeling, and characterization of high performance semiconductor devices and integrated circuits with MOSFETs, HEMTs & HBTs, and nanostructure quantum effect devices. He also works on the development and application of the photonic and optoelectronic microwave technique for the characterization of physical mechanisms in semiconductor devices.